Electromagnetic and Computational Approach to Detect Depth of the Buried Object Using Radar Remote Sensing Data at X – band

D. Singh

Department of Electronics & Computer Engineering, Indian Institute of Technology Roorkee, Roorkee-247667, (U.A) India, E-mail: dharmfec@iitr.ernet.in

***Abstract*— Present paper deals the fusion of image analysis with electromagnetic and least square (LSE) optimization approach to estimate the depth of shallow buried metallic and dummy mine (i.e., without explosive) objects with microwave remote sensing data at X-band (i.e., 10 GHz). The objects were buried under dry and smooth sand. For this purpose, a monostatic scatterometer at X-band has been indigenously developed, which consists a transmitter and receiver mounted on the stand of the sand pit and when operated it moves over it in X- and Y- axis. An algorithm has been proposed for identification of suspected region first i.e., region of interest (ROI) that contains buried objects in the image by proposing a quantity "detection figure" (D), which further proceed for depth estimation of buried objects. Algorithm includes image processing, electromagnetic multi layer interaction and LSE approach. The convolution-using image processing techniques has been applied to avoid the overlapping of the return signal. The least square optimization (LSE) approach has been analyzed for estimation of depth and an efficient method based on electromagnetic multiplayer interaction concept has been proposed for LSE. The depth estimated for Al sheet gives better result than dummy landmine, but the estimated depths results for both objects are in good agreement with actual depths. The present approach may be quite helpful to develop an automatic satellite data based information systems to estimate the depth of various shallow buried objects with satellite or air-borne radar data.**

***Index Terms*— Shallow buried objects, Image Analysis, Monostatic Scatterometer**

I. Introduction

DETECTION of buried objects has attracted attention of researchers in variety of fields including military, archeology, criminology, and geophysical exploration. Microwave radar is known to be the most likely answer to these detection problems.

Over the years, much of work is done in the retrieval of the buried objects and landmines. One of such autonomous system [1] is developed for detection of subsurface buried objects; this system automatically detects and also can remove the object. Other system include microwave imaging of multiple cylinders using local shape functions [2] and time domain radar system [3] which uses the time averaging and time gating techniques to suppress the noise level, while the time domain approach is also employed with the combination of the Finite Difference Time Domain (FDTD) and matched filter [4] and other includes detection of buried objects equipped with neural network and pattern recognition approach [5]. Systems based on Fuzzy logic are developed for unexploded ordinances [6] and steepest descent fast multipole approach for electromagnetic scattering from penetrable/PEC objects under rough surface [7] while Hulay et al 2004 [8] uses surface impedance concept for detection and determining the location of Buried Objects. Multi-Source strategy based on a learning-by-examples technique for buried object detection is used by Bermani et al 2005 [9] and most recent one is a optimization approach based on SVM for electromagnetic subsurface sensing in which instead of the object localization, the region of interest is divided into free areas and UXO populated areas [10]. The ground penetrating radars suffer from the limitation of 3D resolution and the ground clutter. Therefore, some of the approaches based on SAR are developed.

Considering the problem of detecting buried objects with the help of data obtained by radar, there is the possibility of larger number of false alarms due to stones, tree roots etc. Some method is needed which can identify the suspected region (ROI) in the image, which contains buried objects. Various image-processing techniques have found extensive use and have increased the confidence in identification of ROI. However these techniques are found to be ineffective when signal to noise ratio is poor [11].

Maximum approaches described here are either very complex or need a huge amount of data and limitations of these models are that the inversion of parameters which is only depending upon the number of the datasets. With the need of the retrieval of parameters with less number of datasets, search of the optimization techniques started.

The paper is organized in such a way that, section 2 deals the methodology, which includes system overview and details

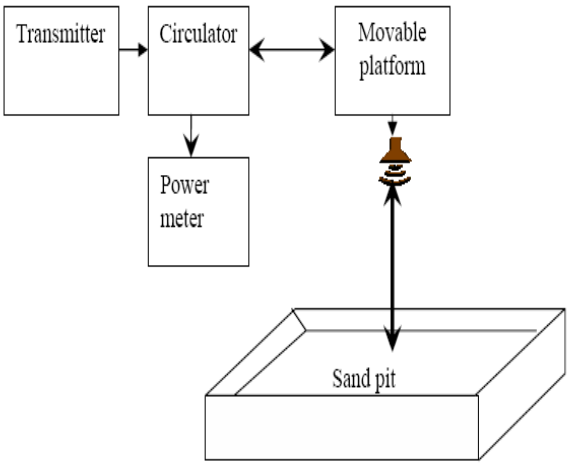

Fig. 1. Schematic diagram of Monostatic Scatterometer.

of proposed approach. Experimental measurements and depth estimation with experimental data is discussed in section 3 followed by the concluding remarks in section 4.

II. METHODOLOGY

A. *System Overview*

A monostatic Radar (scatterometer, shown in fig. 1) has been assembled for the detection of buried object. We have measured the backscattered intensity from the surface for plane polarized (Horizontal-Horizontal; HH- polarization) at normal incidence and at frequency of 10.0 GHz. A pyramidal Horn, which, have E-plane, and H-plane half power beam widths 18.0° and 19.5°, respectively with a gain of 20.27 dB is used for transmitting as well for receiving the backscattered intensity. The system is mounted over 1. 5 m height from the sand-pit on the movable platform which scans the region of interest in steps of 2.0 cm in the two dimensional plane. The surface scanning for scattered response used a grid of 2cm x 2cm in the X-plane and Y-plane on the test bed. These objects were buried at the center of the sandpit with dimension 2.5m x 2.5m. The different sizes of the aluminum sheet (30x30, 24x61, 37x61 cm^2) and dummy land mines (without explosive, size 30x20 cm^2) had been put at different depths (i.e., 0.5 cm, 1.0 cm to 11 cm at the interval of 1.0cm). The same sample was kept at different depths into the sandpit. Adequate care was taken every time in filling the sand pit and leveling it up. The surface was smooth and sand was dry. The calibration of the system was carried out with flat aluminum sheet putting over the sand pit, before each scan with a view to ascertain the truthfulness of data collected for each test objects [12]. The images were constructed from the raw data and then calibration has been carried out.

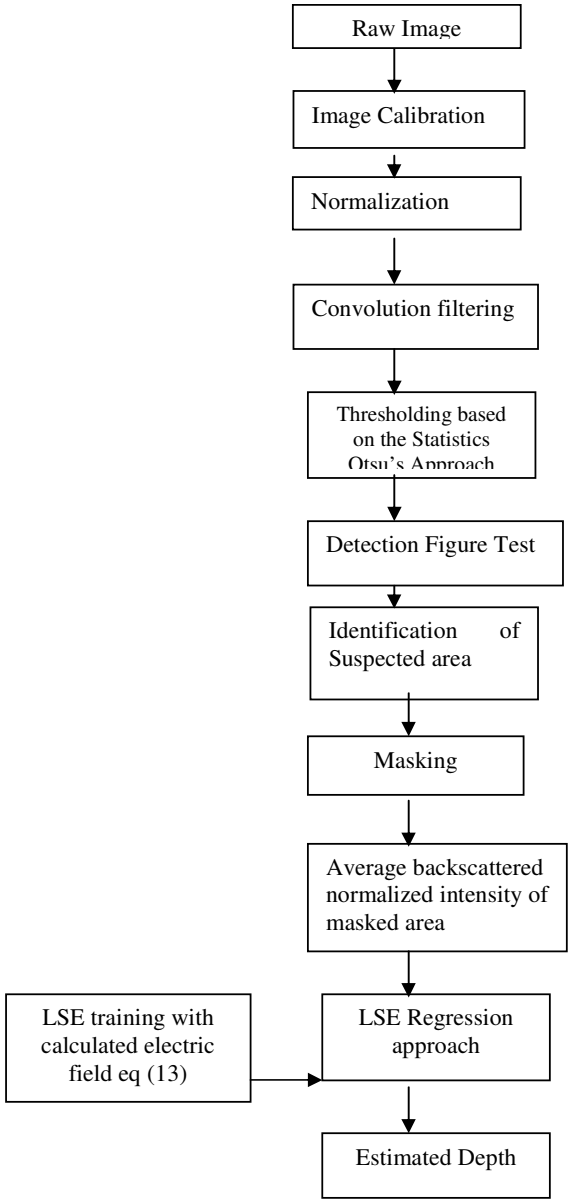

Fig. 2. Flow chart of proposed algorithm.

B. *Algorithm Overview Based on Image Processing with Electromagnetic (EM) and LSE Approach for Depth Estimation of Shallow Buried Metallic/Dummy Mines Objects*

The flow chart of algorithm is given in fig. (2) and details are discussed in following sections.

1) Calibration: Proper care has been taken to calibrate the system and it is performed by putting a rectangular aluminium sheet of same size of sand pit and observation were taken for aluminium sheet before observations of sand pit with buried objects [22].

2) Normalization of image: The raw image were calibrated and after that normalized with the eq. (1)

$$E_{normalised} = \frac{E_{observed} - E_{min}}{E_{max} - E_{min}} \quad (1)$$

Where E_{max} and E_{min} are the maximum and minimum values in the observed data and $E_{observed}$ is backscattered intensity at particular point. The normalization has been done to put all the data in one range.

3) Application of convolution filter: The illumination area of the antenna system is not limited to the pixel size of the image, so there is a significant contribution from the neighboring pixels. Therefore, before proceeding further, care should be taken to minimize the effect of overlap the scattered field from neighbors. For this purpose, convolution filter has been applied to reduce the effect of the overlapping of the scattered field and the random noise spikes in the image with the optimized kernel using Matlab codes.

4) Thresholding based on Otsu's Method [13]: To obtain the suspected area where object may be buried, it is very important to select proper threshold value, say 't'. Each threshold determines a variance for the group of values greater than or equal to t and a variance for group of values less than t. The definition for best threshold suggested by Otsu, 1979 [13] is that the threshold should be selected as the one for which weighted sum of group variances is minimized. The weights are the probabilities of respective groups. This criterion emphasizes high group homogeneity.

5) Detection Figure for minimizing the false alarm: For reduction of the false points, a quantity Detection Figure (D) has been proposed, which is based on image statistics. After thresholding, from mean reading for foreground pixels (those pixels for which reading is above or equal to threshold), mean reading for background pixels (those pixels for which reading is below threshold) and mean reading for the whole data, it is possible to predict confidently whether sand pit has an object buried or not by proposing a quantity "detection Figure".

The detection figure can be defined as,

$$\text{Detection figure} = \frac{\text{A(FG) - A(BG)}}{\text{A(FG + BG)}} \times 100 \quad (2)$$

Where, A (FG) = average reading for foreground pixels,
A (BG) = average reading for background pixels,
A (FG+BG) = average reading for all pixels.

The detection figure has been calculated for different depth of aluminum sheet and dummy landmine. For each depth; minimum, maximum and average values of detection figure were calculated. When there is no object buried into sandpit all readings represent backscattering from sand, hence difference between A (FG) and A (BG) will be small and detection figure will have small value. It was found that if detection figure obtained is less than 40, we could claim that there is no object buried up to a depth of 11 cm in sand.

6) Masking for identification of suspected region (ROI):

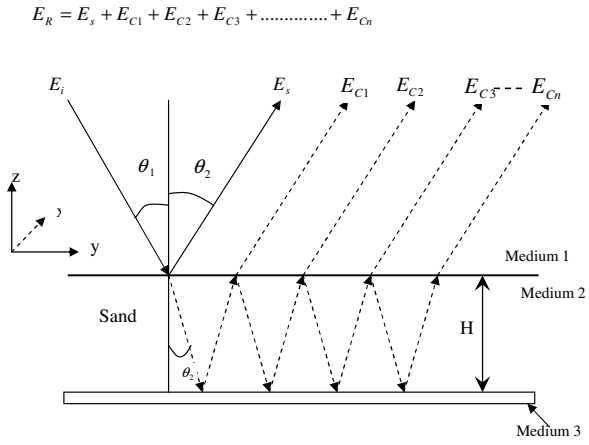

Fig. 3. Electromagnetic interaction with multiple media.

After applying thresholding and detection figure test, mask has been generated and average backscattered intensity of masked region has been obtained for further optimization of depth with LSE.

7) LSE Regression Approach for Depth Determination: For the determination of depth, we have performed the inversion via a regression-based LSE approach. The LSE optimization has been done by electromagnetic modeling as given in eq. (13) and discussed in section II B.8. The E_N with eq. (13) has been calculated for the depth 0.0 to 50 cm at the interval of 0.1 cm to optimize the LSE. Then scaling on the training data as well as on test data has been applied that is followed by the cross-validation for best parameter search (i.e., depth).

8) Electromagnetic Modelling Approach for depth estimation with LSE

The total returned electric field at the scatterometer receiver, E_R, arising from incident electric field, E_I, is the result of simultaneous effect of [14], specular reflections and the diffuse scattering from the air (medium 1)-sand (medium 2) interface, reflection from the buried objects (medium 3) at the depth H under the surface, diffraction and scattering by surface irregularities of the reflector and volume scattering from the inhomogenities of the sand layer (medium 2) (fig.3). We can neglect the diffuse and the diffraction component of the electric field scattered by the buried objects, as it is smooth with respect to the radar wavelength of 3cm. Since the thickness of the buried objects is much greater than the depth of its skin layer, which is of order of micrometer (for Al), its surface can be considered a flat boundary through which there is no further penetration of the electric field in to further sand. Consequently, this model for E_R consist of a homogeneous layer of sand that is located between medium 1 and medium 3 with a flat specularly reflecting boundary at z = -H and a boundary between medium 1 and medium 2 is described by a function h=h(x, y), where h is the variation of the surface height relative to horizontal plane z = 0.

This Electromagnetic wave propagation model assumes that the incoming electromagnetic wave with electrical field E_I is planner, medium 2 is infinite in both directions x and y, and medium 1 and 3 are also effectively infinite in the directions of the z axis and –z axis, respectively. The resulting electric field E_T can be considered as the superposition electrical fields [14] (i.e., The returned electric field at the air sand interface E_S, the returned electric field after one reflection at the aluminum/dummy land mines reflector E_{C1}, and returned electric field after two or more reflections at the buried objects and at the air sand interface, E_{C2} and so on).

So the corresponding expressions for the electric field components, if E_I =1 are as following

$$E_S = R_{1-2} \tag{3}$$

$$E_{C1} = T_{1-2} R_{2-3} T_{2-3} \, exp(-2\gamma_2 H) \tag{4}$$

$$E_{C2} = T_{1-2} R_{2-1} T_{2-1} \, exp(-4\gamma_2 H) \tag{5}$$

On summing all the components of the electric, and with E_I =1 one can obtain the following equation

$$R = R_{1-2} + T_{1-2} T_{2-1} \sum_{m=1}^{m=N} R_{2-3}^{m} R_{2-1}^{m-1} \, exp\left(-2\gamma_2 H\right) \tag{6}$$

Where R_{1-2} is Fresnel's reflection coefficient for the air-sand interface, R_{2-3} is Fresnel's reflection coefficient for the buried objects, T_{1-2} is transmission coefficient at the air-sand interface, T_{2-1} is transmission coefficient at the sand-air interface and γ_2 is the propagation constant of the incident wave in sand which basically depends upon the permittivity of sand. The Fresenel's reflection coefficient and transmission coefficient for horizontal polarization at normal incidence angle is given as

$$R_{1-2} = \frac{\eta_2 - \eta_1}{\eta_2 + \eta_1} \tag{7}$$

$$R_{2-3} = \frac{\eta_3 - \eta_2}{\eta_3 + \eta_2} \tag{8}$$

$$T_{1-2} = \frac{2\eta_2}{\eta_2 + \eta_1} \tag{9}$$

$$T_{2-1} = \frac{2\eta_1}{\eta_1 + \eta_2} \tag{10}$$

η_i is characteristic impedance of the ith medium and depends upon the permittivity of the medium. The R is sum of convergent series and as m tends to infinite, it can be given by [25]

$$R = \frac{R_{1-2} + R_{2-3} \, exp\left(-2\gamma_2 H\right)}{1 + R_{1-2} R_{2-3} \, exp\left(-2\gamma_2 H\right)} \tag{11}$$

Final expression for the total returned electrical field at scatterometer receiver, E_R (which is called calculated) for a buried object at depth H under the a smooth sand layer

$$E_R = \frac{R_{1-2} + R_{2-3} \, exp\left(-2\gamma_2 H\right)}{1 + R_{1-2} R_{2-3} \, exp\left(-2\gamma_2 H\right)} \tag{12}$$

The dependence of R on H has been numerically analyzed and it was found the oscillatory behavior. This calculated electric field is then normalized as following equation

$$E_N = \frac{E_R - E_{R\_min}}{E_{R\_max} - E_{R\_min}} \tag{13}$$

where E_R is the calculated electrical backscatter field at a given buried object depth, E_{R_max} is the maximum calculated backscatter electric field, E_{R_min} is minimum calculated backscatter electric field and E_N is the calculated normalized backscatter electric field.

Using Eq. (13), we can compute the normalized backscatter electric field at any depth H, which can be used for optimize the LSE for depth estimation. The E_R gives the value of calculated electrical backscatter coefficient and it is clearly seen that it is a function of dielectric constant of the mediums and depth (H).

$$E_R(\theta) = f(\varepsilon,\theta).f(H,\theta) \tag{14}$$

The dielectric constant of the medium is assumed constant during whole measurement, so it can be written as

$$E_R = \xi.f(H,\theta) \tag{15}$$

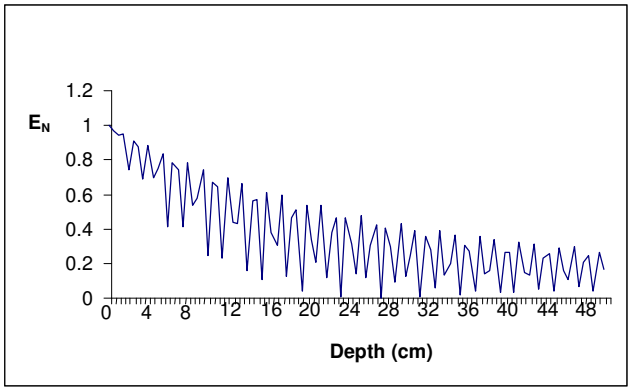

Fig. 4. Calculated Normalized backscattered Electric field with depth of buried object (Aluminum) sheet.

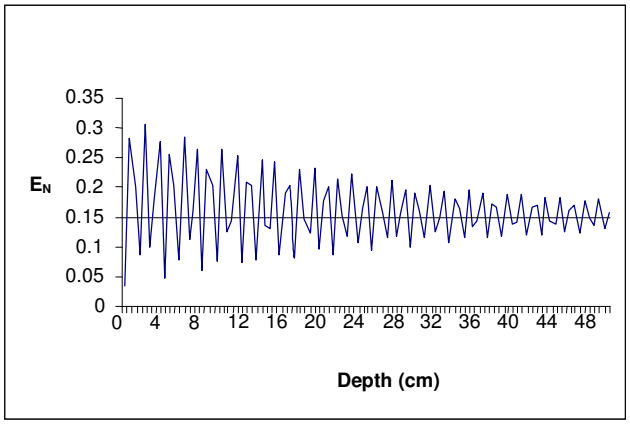

Fig. 5. Calculated Normalized backscattered Electric field with depth of buried object (Teflon) sheet.

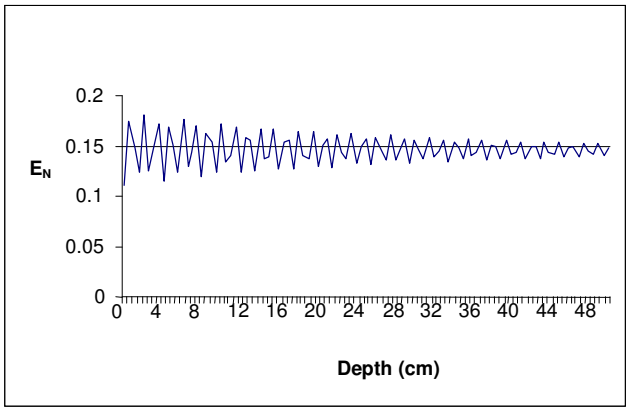

Fig. 6. Calculated Normalized backscattered Electric field with depth of buried object (Bakellite) sheet.

Where ξ is a dielectric constant dependent parameter and in our case it is constant. This calculated electrical backscatter coefficient is used for the Non Linear Least Square Optimization computational technique for estimating the depth of buried object with the measured electrical backscattering coefficient by the scatterometer as represented in equation (4),

$$\text{Minimize} = \sum \left[\left\{ \left(\frac{1}{\lambda_1^2} \right) \cdot \left(E_{R\_obs} - E_{R\_cal} \right)^2 \right\} + \left\{ \left(\frac{1}{\lambda_2^2} \right) \cdot \left(H_{obs} - H_{est} \right)^2 \right\} \right] \quad (16)$$

Where λ_1^2 standard deviation of measured E_{R_obs} at 0° incidence angles

E_{R_obs} = electrical backscattering coefficient observed during experiment at 0° incidence angle.

E_{R_cal} = electrical backscattering coefficient calculated by equation (1)

λ_2^2 = Standard deviation of the observed (*a priori*) depth (H_{obs})

H_{obs} = Depth of buried object (*a priori* information or guess value) observed during experiment.

H_{est} = Depth to be retrieved (i.e., estimated).

For estimation of $H_{est,}$ known values of other parameter i.e. λ_1^2, E_{R_obs}, E_{R_cal}, λ_2^2, and H_{obs}, were inserted into a computer program using software and it gives the values of H_{est}.

Calculated normalized backscatter electric field with depth is shown in figs (4-6) for aluminum sheet, teflon and bakelite respectively. The dielectric constant for sand 4.2, bakelite 5.0 and Teflon 2.0 [15] were considered for computation of backscattered electric field. It is clearly observed in all three figures that nature of E_N is oscillatory and Al sheet gives more back scattered electric field than the other low dielectric materials. Usually landmines are prepared by very low dielectric constant materials.

III. Experimental Measurements and Depth Estimation

To identify the suspected region (ROI) and for depth estimation of buried objects, we have taken various size of the aluminum sheet and one dummy mine (without explosive) of size 30 by 20 cm^2. Objects were buried into sand pit at different depths (0.5 cm to 11 cm at the regular interval of 1.0 cm) and observations were taken by monostatic scatterometer at X-band. The sand pit was scanned at the interval of 2 cm at X- and Y-axis. Mainly three types of observations were taken

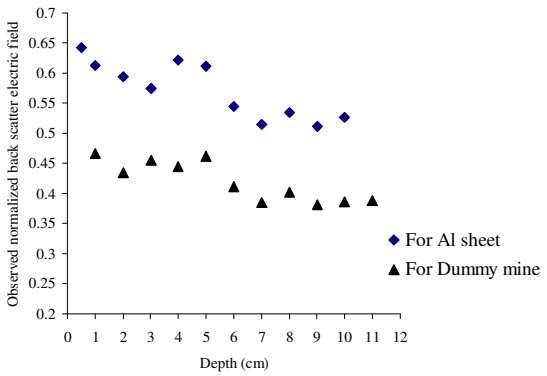

Fig. 7. Observed normalized backscattered electric field for Al sheet and dummy mine at different depths.

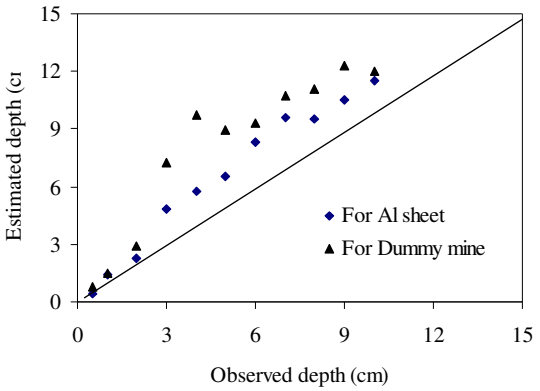

Fig. 8. Estimated depth and observed depth.

(i.e., (i) with aluminum sheet which covered the entire sand-pit for calibration purpose, (ii) for sand-pit only for observing clutter distribution and to cross validate the thresholding and (iii) for aluminum sheet of different sizes and dummy landmine at different depths. Then, the proposed algorithm as discussed in section (2) has been applied on the raw image and suspected region (ROI) has been masked. For example, for aluminum sheet of size (30 X 30 cm^2) and buried at the depth of 6cm. Raw image were generated from the scatterometer data and normalized as eq. 1 (max=9.7724, min=2.4547) after that convolution filter into the normalized image were applied. Then threshold approach based on the Otsu [13] (mean = 0.0653, standard deviation = 0.1510) has been applied for identification of suspected region. The ROI were checked by detection figure and for this Al sheet, we got D is equal to 75.6 and for dummy mine D was found 61.4 percent that is quite above with the detection threshold and we can proceed for masking the ROI. The normalized backscatter electric field of this masked region was further used for depth prediction. Similar procedure has been adopted for processing all the data. The observed normalized backscattered electric field with various depths for one Al sheet of above said size and dummy mine is shown in fig (7). The variation of observed $E_{Normalized}$ is quite evident for both objects. The LSE result for depth estimation is shown in fig (8) for Al sheet and dummy mine. Quite good agreement between actual depth and estimated depth has been noticed for both objects. But, depth estimation for Al sheet (R^2=0.97) gives better result than dummy mines (R^2=0.86). It is also clearly observed that the depth till 5 cm can be very closely estimated. Similar results were obtained for various sizes of used Al sheets.

IV. Conclusion

An algorithm based on EM and image analysis approach has been proposed for detecting and depth estimation of shallow buried objects. The proposed detection figure quantities give quite encouraging results which can be applied and checked in the satellite images. The proposed EM approach for LSE seems to be quite efficient and produced good results. More work has to be done in near future for different terrain conditions (i.e., roughness and moisture). This type of work will be quite helpful in near future to develop information system for radar data to identify the shape of shallow buried objects, which can also be applied to satellite remote sensing.

Acknowledgment

Author is thankful to ARMREB, Defence Research Development Organization of India to provide financial support for this work. Author is also thankful to Prof. K. P. Singh, Department of Electronics Engineering, Institute of Technology, Banaras Hindu University, Varanasi, U.P., India for technical discussion and Mr. Ananad Swami for conducting the experiment.

References

[1] H. Herman, S. Singh, "First result in the autonomous retrieval of buried Objects" *International conference on Robotics and Automation*, May 1994, San Diego.

[2] W. C. Chew, A. Gregory, and P. Otto, "Microwave imaging of multiple conducting cylinders using local shape functions" *IEEE Microwave and Guided wave letters*, vol. 2, no. 7, pp. 156-162, 1992.

[3] W. C. Chew, and G. Otto, "Microwave imaging of multiple cylinders using local shape functions" *IEEE Transaction on Microwave Theory and Techniques*, vol. 42, no. 1, pp. 235-242, 1994.

[4] T. Dogaru, and L. Carin, "Time-Domain sensing of targets buried under a rough air–ground interface" *IEEE Transactions on Antennas and Propagation*, vol. 46, no. 3, pp. 678-685, 1998.

[5] W. Al-Nuaimy, Y. Huang, M. Nakhkash, M. T. C. Fang, V. T. Nguyen, and A. Eriksen, "Automatic detection of buried utilities and solid objects with GPR using neural networks and pattern recognition" *Journal of Applied Geophysics,* vol. 43, pp. 157–165, 2000.

[6] L. M. Collins, Y. Zhang, J. Li, H. Wang, L. Carin, S. J. Hart, L. Susan Rose-Pehrsson, H. Herbert Nelson, and J. R. McDonald, "A comparison of the performance of statistical and fuzzy algorithms for unexploded ordnance detection" *IEEE Transactions on Fuzzy Systems*, vol. 9, no. 1, pp. 281-288, 2001.

[7] M. El-Shenawee, "Polarimetric scattering from two-layered two-Dimensional random rough surfaces with and without buried objects" *IEEE Transactions on Geosciences and Remote Sensing*, vol. 42, no. 1, pp. 742-752, 2004.

[8] A. H. Hulay, A. Yapar, and I. Akduman, "Use of surface impedance in the detection and location of buried objects" *International Journal of Electronics and Communication,* vol. 58, pp. 166-172, 2004.

[9] E. Bermani, A. Boni, A. Kerhet, and A. Massa, "Kernels evaluation of LSE-based estimators for inverse scattering problems" *Progress In Electromagnetics Research, PIERS*, vol. 53, pp. 167–188, 2005.

[10] A. Massa, A. Boni and A. Donelli, "Classification approach based on LSE for Electromagnetic Subsurface Sensing" *IEEE Trans. on Geosci. and Remote Sensing*, vol. 43, no. 9, pp-246-253, 2005.

[11] V. Chandrashekhar, "*Edge Detection and Eerror Analysis of Scatterometer Data*," M. Tech. Thesis, Dept. of Electronics Engg. I.T., B.H.U., Varanasi. India, 1997.

[12] F. T. Ulaby, R. K. Moore and A. K. Fung, "Microwave remote sensing-active and passive" *Addison Wesley,* Vol. 1, 2 and Vol. 3, 1982.

[13] N. Otsu, "A thresholding selection method from grey level histogram", *IEEE Trans. On Systems, Man and Cybermatics*, vol. 9, pp. 62-66, 1979.

[14] Julian Daniels, Dan G. Blumberg, Leonid D. Vulfson, Alex L. Kotlyar, Valentin Freiliker, Gefen Ronen, Jiftah Ben-Asher, "Microwave remote sensing of physically buried objects in the Negev Desert: implications for environmental research", *Remote Sensing of Environment*, vol. 86, pp. 243–256, 2003.

[15] http://www.clippercontrols.com/index.html